CYCLING ATTRACTORS OF COUPLED CELL SYSTEMS AND DYNAMICS WITH SYMMETRY

PETER ASHWIN*
School of Mathematical Sciences, Laver Building, University of Exeter, Exeter EX4 4QE, UK

ALASTAIR M. RUCKLIDGE †
Department of Applied Mathematics, University of Leeds, Leeds LS2 9JT, UK

ROB STURMAN‡
Department of Applied Mathematics, University of Leeds, Leeds LS2 9JT, UK

Abstract. Dynamical systems with symmetries show a number of atypical behaviours for generic dynamical systems. As coupled cell systems often possess symmetries, these behaviours are important for understanding dynamical effects in such systems. In particular the presence of symmetries gives invariant subspaces that interact with attractors to give new types of instability and intermittent attractor. In this paper we review and extend some recent work (Ashwin, Rucklidge and Sturman 2002) on robust non-ergodic attractors consists of cycles between invariant subspaces, called 'cycling chaos' by Dellnitz et al. (1995).

By considering a simple model of coupled oscillators that show such cycles, we investigate the difference in behaviour between what we call *free-running* and *phase-resetting* (discontinuous) models. The difference is shown most clearly when observing the types of attractors created when an attracting cycle loses stability at a resonance. We describe both scenarios – giving intermittent *stuck-on* chaos for the free-running model, and an infinite family of periodic orbits for the phase-resetting case. These require careful numerical simulation to resolve quantities that routinely get as small as 10^{-1000}.

We characterise the difference between these models by considering the rates at which the cycles approach the invariant subspaces. Finally, we demonstrate similar behaviour in a continuous version of the phase-resetting model that is less amenable to analysis and raise some open questions. [1]

[1] (2003) In *Synchronization: Theory and Application* A. Pikovsky and Y. Maistrenko (eds), Kluwer: Dordrecht, 5–23.

1. Introduction

To understand more complex dynamical systems, it is often helpful to break them down into a number of smaller units or 'cells' that interact with each other. These cells may be imposed naturally by the system one is modelling (for example, neuronal activity), or may just be mathematically helpful (such as linear spatial modes in a spatially extended nonlinear system). Isolating the interactions between the units and the dynamics of the individual units gives a coupled cell description for the dynamics. A basic question for such systems is whether the attracting dynamics of the system is synchronized in any sense.

In cases where the cells are identical the dynamics is constrained by the existence of invariant (synchronized) subspaces for the dynamics. The paper reviews some recent work that exploits symmetries of coupled identical cell systems to help understand their generic behaviour.

The paper proceeds as follows. In section 2 we review some basic concepts from dynamical systems with finite symmetry group and the effects of invariant subspaces. In section 2.1 we discuss the stability and bifurcation of attractors in and near invariant subspaces; a common feature of such attractors is that they may be highly intermittent (Ashwin, 1999).

In section 2.2 we discuss a class of more complicated intermittent attractors that nevertheless *robustly* appear, that involve a number of invariant subspaces. These attractors have dynamics that show 'cycling chaos' (Dellnitz et al., 1995) between a number of invariant sets that may be chaotic or periodic. These attractors may be non-ergodic, namely there are obstructions to convergence of averages of observations made on the system.

For the remainder of this article we focus on a particular family of coupled systems introduced in (Ashwin et al., 2002) that have robust cycling attractors. Section 3 introduces these cyclically coupled logistic maps, and if we ensure (by introducing a discontinuity in the map) that the approach to consecutive chaotic saddles is via a single trajectory (we call this phase-resetting) we can investigate how their instability causes the appearance of an infinite family of nearby periodic orbits. Finally we present in section 3.5 evidence that phase-resetting can appear even if the map remains smooth.

* P.Ashwin@ex.ac.uk
† A.M.Rucklidge@leeds.ac.uk
‡ rsturman@amsta.leeds.ac.uk

2. Dynamics with symmetry

Rich dynamics are frequently found in systems that commute with a group of symmetries. These symmetries constrain what can happen in the system while also causing atypical behaviour to become generic. At the simplest level, symmetries cause multistability of attractors; any symmetric image of an attractor must also be an attractor. Moreover, if an initial condition has a certain symmetry, this symmetry must be retained along the trajectory giving rise to invariant subspaces for the dynamics. Symmetries can also cause constrain instabilities by forcing repetition of eigenvalues or Lyapunov exponents corresponding to perturbations that are in symmetrically related directions.

The development of equivariant dynamical systems, or dynamical systems with symmetry, has made great progress in giving a number of tools from group representation and singularity theory to classify such behaviour. This has been particularly successful in classifying local bifurcations of equilibria and periodic solutions (see Golubitsky et al. 1985, 1988, 2002) but in this article we do not discuss this or its application to coupled cell networks.

2.1. ATTRACTORS IN INVARIANT SUBSPACES AND INTERMITTENCY

For dynamics that is symmetric under linear actions of a finite group, there is a linear invariant subspace associated with each subgroup of symmetries. When an attractor in an invariant subspace loses transverse stability due to a change of parameter we have a so-called *blowout* bifurcation. More precisely, consider a dynamical system on $\mathbb{R}^n$, containing an subspace M of dimension $m < n$ which is invariant under the action of the system. Suppose that for parameters μ below a critical parameter μ_c the subspace M contains a chaotic attractor A of the full system. A blowout bifurcation occurs at μ_c if A ceases to be an attractor for $\mu > \mu_c$. Two different types of blowout bifurcation scenario were characterised in (Ott and Sommerer, 1994) and applications to coupled systems noted in (Ashwin, Buescu and Stewart, 1994). The first scenario is *subcritical* (also called *hysteretic* or *hard*) and occurs when there are no nearby attractors beyond the bifurcation. This class of blowout is characterised by a riddled basin of attraction. The second is the *supercritical* (also called *nonhysteretic* or *soft* case), in which on-off intermittent attractors branch from the original attractor when the bifurcation parameter increases; for a review of intermittency effects see (Ashwin, 1999).

Despite the complexity and diversity of the dynamics in such cases, the resulting attractors are generally observed to have ergodic natural measures as far as one can tell from numerical simulations. This seems is true for

generic attractors that arise in dynamical systems and means that average quantities (such as Lyapunov exponents) can be computed from attracted trajectories and are natural in the sense that they are the same for almost all initial conditions. One of the most surprising results from the study of symmetric systems is that attractors without ergodicity can be found in fairly simple symmetric systems and moreover these can be robust to (symmetry-respecting) perturbations. A review of these robust heteroclinic cycles can be found in (Krupa, 1997) and a classification of more general heteroclinic networks that may arise in symmetric systems can be found in (Ashwin and Field, 1999).

2.2. CYCLING ATTRACTORS

One of the best-known non-ergodic attractors is the structurally stable heteroclinic cycle between fixed points in $\mathbb{R}^3$ (the "Guckenheimer and Holmes cycle", (Guckenheimer and Holmes, 1988)). This is given by the equation

$$\begin{aligned} \dot{x} &= x(l + ax^2 + by^2 + cz^2) \\ \dot{y} &= y(l + ay^2 + bz^2 + cx^2) \\ \dot{z} &= z(l + az^2 + bx^2 + cy^2). \end{aligned} \tag{1}$$

For the system (1) the coordinates planes, the diagonals $x(\pm 1, \pm 1, \pm 1)$ and the axes are all invariant. Moreover, there is an open set of parameters (a, b, c) such that all trajectories off these invariant subspaces approach a robust cycle formed from three equilibrium points on the coordinate axes and trajectories in the coordinate planes connecting these points. Although heteroclinic cycles are possible in systems without symmetry, they are not structurally stable unless there are constraints on the system. The presence of invariant subspaces means that the cycle can be robust – that is, stable with respect to perturbations which preserve invariance of the coordinate planes.

This heteroclinic cycle, illustrated in Figure 1, is robust simply because within the invariant subspaces, the connections are generic connections from saddle to sink. A typical trajectory approaching the cycle will switch between neighbourhoods of the equilibrium points progressively getting closer to the cycle. One can calculate that it will spend a geometrically increasing amount of time close to each equilibrium point and because of this the ergodic averages will be dominated by the present equilibrium and fail to converge. Rather, they will oscillate for ever (Sygmund, 1992; Hofbauer and Sygmund, 1992; Gaunersdorfer, 1990). On varying a parameter in such a system, several mechanisms whereby robust attracting cycle can be created and destroyed have been identified.

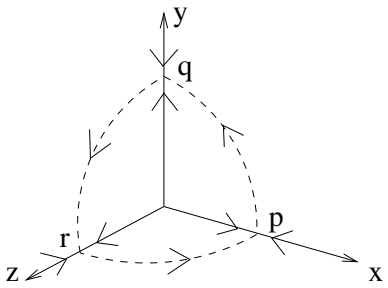

Figure 1. An example of a robust heteroclinic cycle; the Guckenheimer-Holmes cycle in $\mathbb{R}^3$. This is a cycle of heteroclinic connections between the equilibria p, q, r as illustrated, that exists and is attracting for an open set of parameters (a, b, c). The cycle is structurally stable to all perturbations that preserve the coordinate planes; the connection within each coordinate plane is one from a saddle to a sink.

- A *resonance* bifurcation (Chow et al, 1990) creates a large period periodic orbit at loss of stability of the cycle.
- The fixed points themselves bifurcate in such a way as to destroy the connection, for example at saddle-node or Hopf bifurcations or other transverse bifurcations that may create new longer attracting heteroclinic cycles (Chossat et al. 1997a, 1997b).

Cycles can also exist between sets that are more complicated than simple fixed points but can be created and destroyed in a similar way. For example, if we have cycles between chaotic sets (that is, chaotic saddles – attracting *within* an invariant subspace but repelling in *transverse* directions) we have *cycling chaos*, as discussed in (Ashwin, 1997; Ashwin and Rucklidge, 1998; Dellnitz et al., 1995), an aspect of a phenomenon referred to as *chaotic itinerancy* by (Kaneko, 1998). The stability of such cycles is usually governed by the ratios of Lyapunov exponents at the saddles. Loss of stability can occur at a blowout bifurcation that destroys the set of connections (Ashwin and Rucklidge, 1998) or at a *resonance bifurcation* that corresponds to a resonance of Lyapunov exponents (which occurs when the rates of linear expansion and contraction become equal).

One would like to understand the sort of attractors that are created at a resonance bifurcation. This question was posed and investigated for a specific planar magnetoconvection model with robust cycling chaos in (Ashwin and Rucklidge, 1998). The cycle in this case was between a chaotic saddle, an equilibrium point and their images under symmetries of the problem. Numerical simulations in (Ashwin and Rucklidge, 1998) suggest that the resonance bifurcation creates a large number of periodic attractors that branch from the cycling chaos. By contrast, for the skew-product example of cycling chaos examined in (Ashwin, 1997) the resonance was found to

give rise not to periodic orbits but to a chaotic attractor with average cycling chaos, or to quasiperiodicity that is intermittent ('stuck on') to the cycling chaos.

An initial attempt to reconcile these differences was made in (Ashwin et al., 2002), by introducing the terms *phase-resetting* and *free-running*. For the remainder of this paper we recall this distinction and expand upon the examples in (Ashwin et al., 2002). We use *phase-resetting* to describe a cycle in which the connections between invariant subspaces consist of only a single trajectory (for example, in a flow the connections are one-dimensional, or in a map, they are zero-dimensional). By contrast, *free-running* describes cycles which have a set of many possible connections.

3. Coupled logistic maps

3.1. FREE-RUNNING MODEL

Let $f(x) = rx(1-x)$ denote the logistic map with parameter $r \in [0,4]$ and consider the system introduced in (Ashwin et al., 2002):

$$\begin{aligned} x_{n+1} &= f(x_n)e^{-\gamma z_n} \\ y_{n+1} &= f(y_n)e^{-\gamma x_n} \\ z_{n+1} &= f(z_n)e^{-\gamma y_n}. \end{aligned} \tag{2}$$

This map clearly preserves the coordinate planes defined by $xyz = 0$. Three distinct types of evolution are possible for each variable. For example, consider x: if $z \ll 1$ and $x \ll 1$ then x grows approximately linearly – the *growing* phase. For $z \ll 1$ and $x \approx O(1)$, x evolves according to logistic map dynamics – the *active* phase. Finally if $z \approx O(1)$ the dynamics in the x direction is suppressed by the coupling term – the *decaying* phase. For sufficiently large γ we have a robust cycle between invariant sets. In this state, each variable alternates cyclically between the growing, active and decaying phases. We term a change in the phases a *switch*. More precisely, we say a switch occurs when the growing variable exceeds $\ln r/\gamma$. The number of iterations between switches increases approximately geometrically as trajectories approach the invariant subspaces, and this rate of increase depends on the coupling γ. The rate of increase of switching times approaches zero as γ approaches some critical value from above, which forms the limit of the stability of cycling chaos. This geometric increase is examined in more detail in section 3.3.

For $r < 3$ the cycles are between period one points; as r is increased through period doubling we obtain cycles progressively between periodic orbits and then chaotic saddles. Since numerical simulations of this system

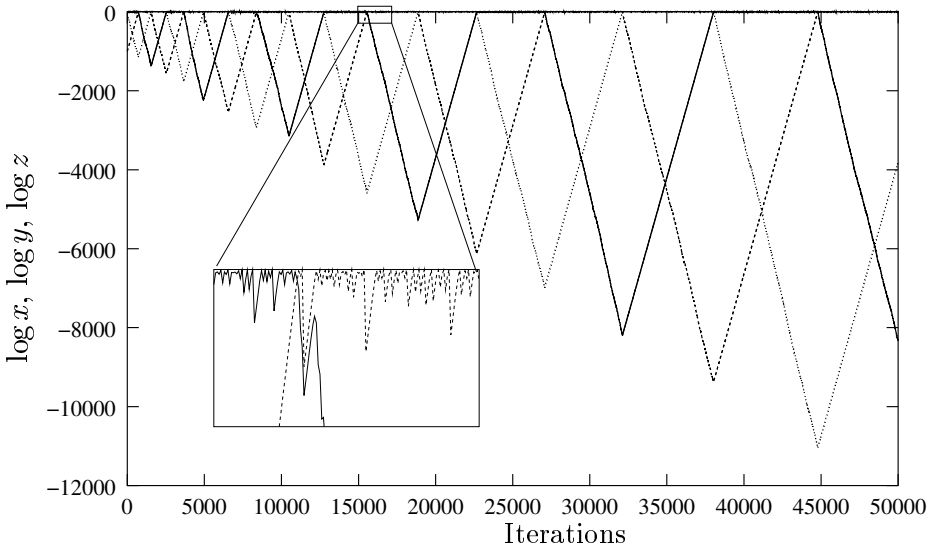

Figure 2. Attracting cycling chaos, with $r = 4.0$, $\gamma = 6.0$. The model is iterated and x, y, z plotted (in logarithmic coordinates) against time. The chaotic behaviour is $O(1)$ and is visible in the inset. The trajectory cycles through growing, active and then decaying phases for each variable, with the length of phase increasing approximately geometrically. (The same behaviour is found for the phase-resetting version discussed in section 3.3.)

need to resolve a neighbourhood of the invariant subspaces at high resolution, we use logarithmic coordinates (Ashwin and Rucklidge, 1998; Pikovsky et al, 2002). The time series in Figure 2 is for parameters that produce attracting cycling chaos. This sort of behaviour could be viewed as a sort of antisynchronization; when one variable becomes active, the currently active variables become quiescent. Referring to Figure 2, decreasing γ results in a slower rate of increase in the number of iterations between switches, and the line formed by connecting the local minima would become more horizontal.

3.2. COMPUTATION OF RESONANCE BIFURCATION

Suppose that cycling chaos loses stability on decreasing γ through a critical value γ_c. We compute γ_c analytically as follows, as shown in (Ashwin et al., 2002). Suppose that the growing variable is z and a switch has just occurred, so $z \ll 1$, x is $O(1)$ and y is decaying. The evolution of z is governed by $z_{n+1} = rz_n(1 - z_n)e^{-\gamma y_n}$, and this can be approximated by $z \to rz$. Starting at a switch at z_0, suppose that the number of iterations until the next switch is N. Then $z_N \approx r^N z_0$, and since z_N is $O(1)$ at a switch, $N \approx -\ln z_0 / \ln r$, where z_0 is the value of z at the start of the growing phase. Whilst z is growing, y is decaying, and for critical γ we

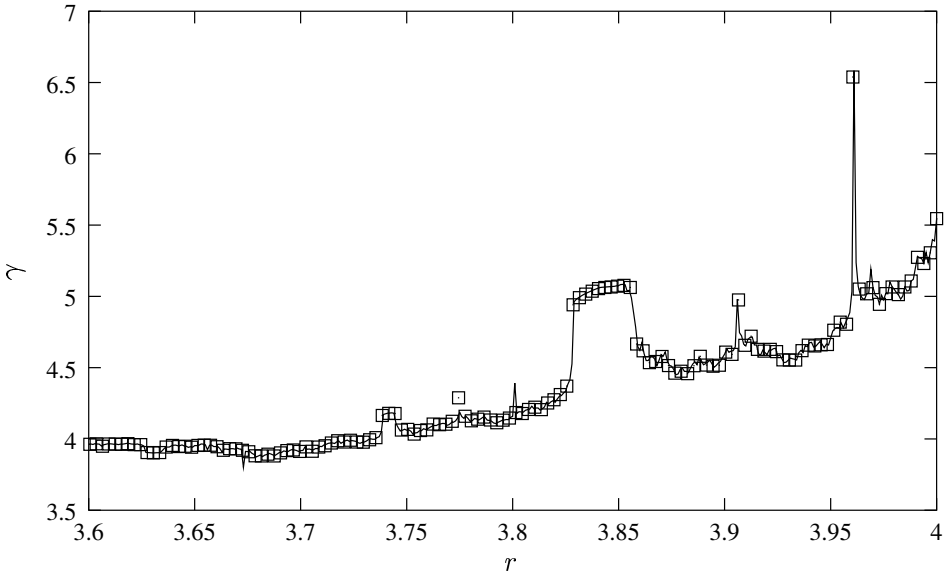

Figure 3. The critical value of γ at which loss of stability of cycling chaos occurs by resonance. The line is estimated using (3) whereas the boxes show points of numerically calculated loss of stability of cycling attractors on varying γ for fixed r. Above the line there is a cycle that is an attractor; below the line the cycling persists but is no longer an attractor.

require $y_N = z_0$. We approximate y_N in a similar way, with y_0 an $O(1)$ number. Throughout the decay phase $y \ll 1$, but it is forced by the active variable x. Here we approximate by $\dot{y} \to ry e^{-\gamma x}$, and replace x by its long-term average A_∞ $(= \lim_{M\to\infty} \frac{1}{M} \sum_i^M f^i(x_0))$ for each of the N iterations, giving $y_N \approx r^N e^{-\gamma N A_\infty}$. Then substituting our expression for N, we have $\ln y_N \approx -\ln z_0 + (\gamma \ln z_0 A_\infty)/(\ln r)$. The critical value of γ occurs when $\ln y_N = \ln z_0$, giving

$$\gamma_c = 2 \ln r / A_\infty. \tag{3}$$

Equivalently, this can be obtained by considering the ratio of the transversely expanding Lyapunov exponent $\lambda = \ln r$ and the contracting Lyapunov exponent $-\mu = \ln r - \gamma A_\infty$. There will be geometric slowing down with asymptotic rate R, where R is

$$R = \frac{\mu}{\lambda} > 1. \tag{4}$$

There is a resonance when this quantity is equal to unity, also leading to (3).

The average A_∞ is easy to compute numerically, and so we can obtain a curve of critical γ shown in Figure 3, plotted as a line. We superimpose points computed by seeking the parameter at which the number of itera-

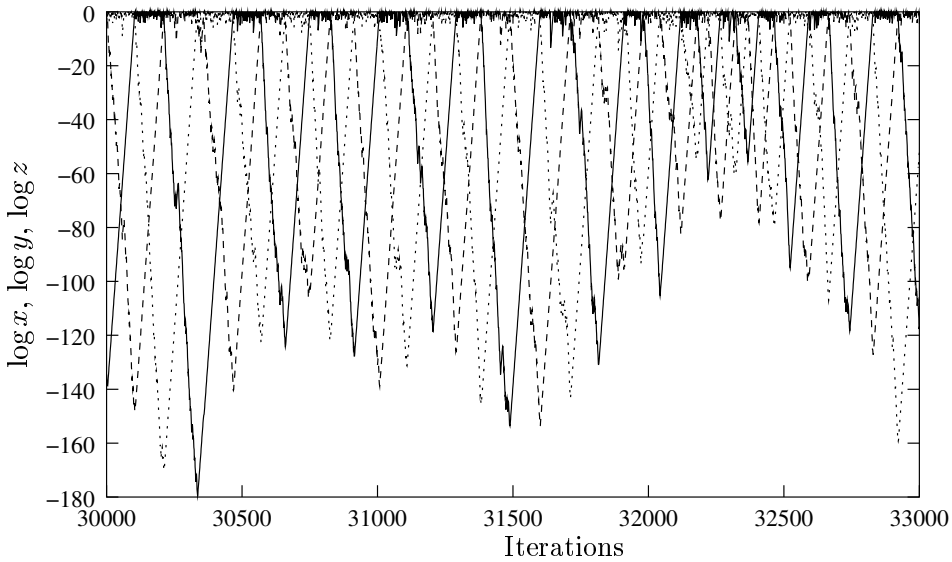

Figure 4. After losing stability at resonance, in the free-running case, the cycle gives way to a stuck-on attractor. Trajectories are intermittent to each invariant subspace, visiting portions of chaotic behaviour in an irregular fashion but with a finite mean time of cycling. $r = 4.0, \gamma = 5.4$.

tions between switches becomes constant, demonstrating the accuracy of the approximation. When the attracting cycle loses stability in a resonance bifurcation, the resulting stable behaviour is stuck-on chaos – that is, a trajectory which cycles irregularly between invariant subspaces, visiting portions of chaotic trajectory in an intermittent fashion. A section of such a trajectory is shown in Figure 4.

This agrees with the conjecture in (Ashwin and Rucklidge, 1998) that in a free-running model, cycling chaos loses stability to stuck-on chaos. Although the connections between invariant subspaces here are one-dimensional, because the model deals with discrete time, it is possible for approaches to chaotic saddles to be along many different trajectories. In order to create a phase-resetting version, and thus hopefully obtain periodic orbits, the logistic map was adapted in (Ashwin et al., 2002) to force the connections to consist of only a single approach trajectory.

3.3. PHASE-RESETTING MODEL

In order to model the phase-resetting observed in a magnetoconvection system in (Ashwin and Rucklidge, 1998), (Ashwin et al., 2002) introduced a phase-resetting enforced by the introduction of a discontinuous 'shelf' in the logistic map. That is, we replace the logistic map f during a growing

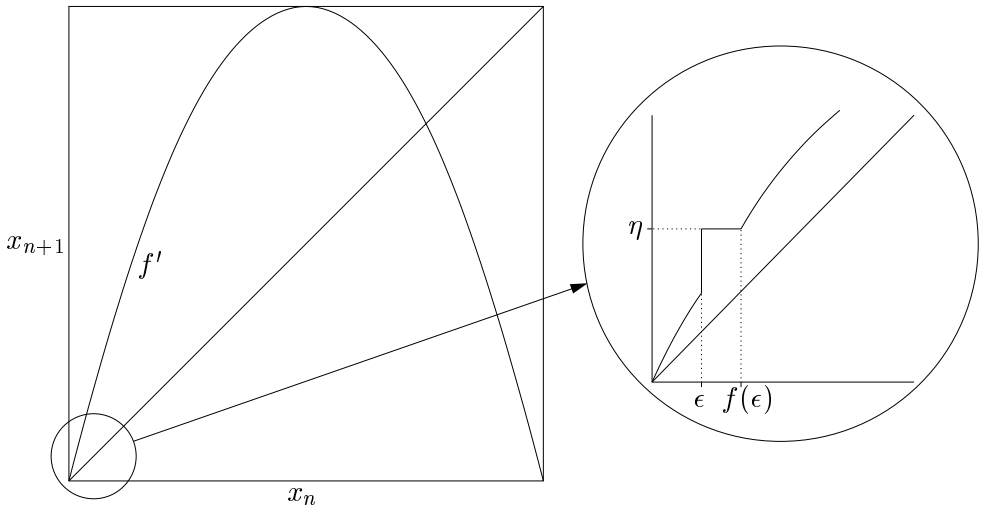

Figure 5. A 'shelf' is introduced to the logistic map. Any iteration falling in $[\epsilon, f(\epsilon)]$ is forced to leave at exactly $\eta = f^2(\epsilon)$. Thus all initial conditions follow the same trajectory into the next saddle.

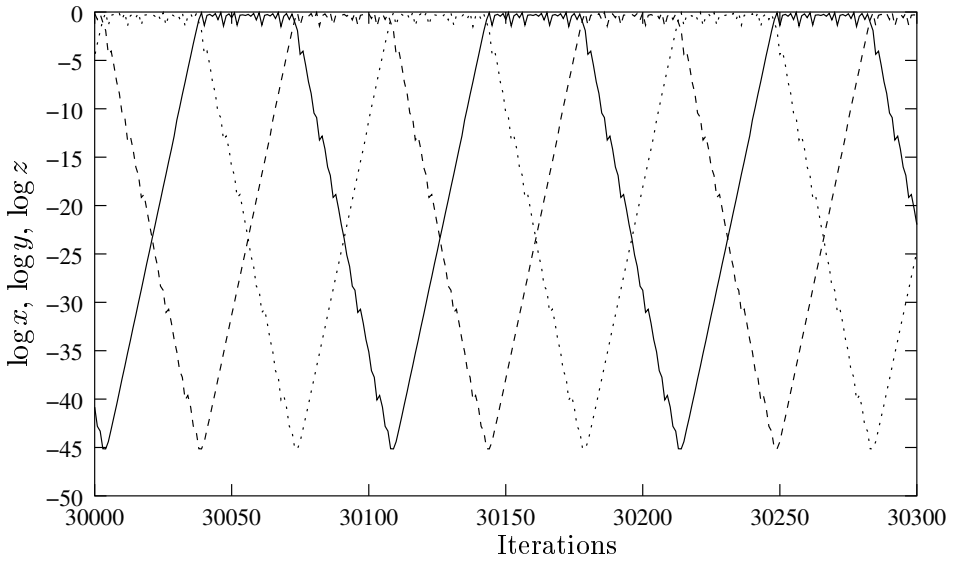

Figure 6. For the phase-resetting case the attracting cycling chaos gives way to many co-existing periodic orbits. The phase-resetting forces each active phase to begin with the same segment of chaotic trajectory.The parameters are $r = 3.75$, $\gamma = 3.9$.

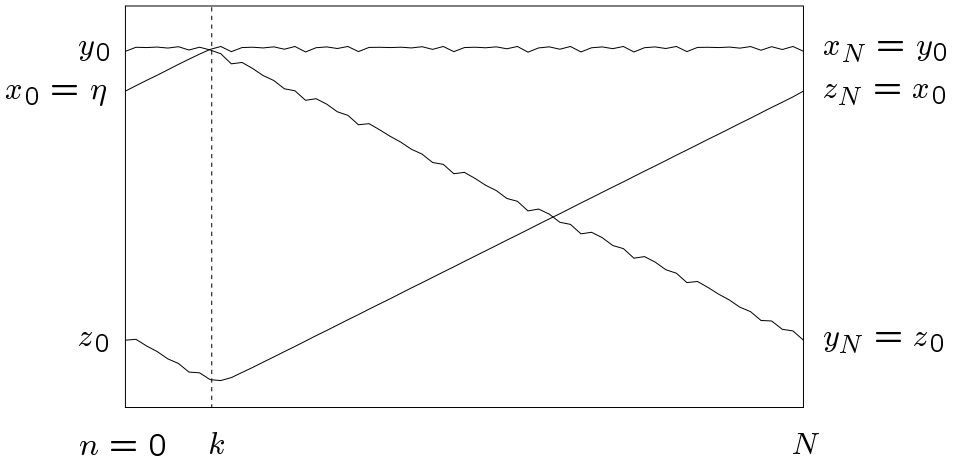

Figure 7. Schematic diagram of a periodic orbit of period $3N$ for the phase-resetting case; one third of a period is shown. This is a periodic orbit as the final and initial phases match up as shown. The iterate k shows where the phases switch.

phase by $\tilde{f}$:

$$\tilde{f}(x_n) = \begin{cases} f(x_n) & x_n < \epsilon \text{ or } x_n > f(\epsilon) \\ f^2(\epsilon) = \eta & x_n \in [\epsilon, f(\epsilon)]. \end{cases}$$

Each time a growing variable reaches the interval $[\epsilon, f(\epsilon)]$ (we use $\epsilon = 10^{-6}$ in the following), it is set to $\eta = f^2(\epsilon)$, as shown in Figure 5. To ensure that $\epsilon < f(\epsilon)$ we now restrict to $r \in [\frac{1}{1-\epsilon}, 4]$.

Attracting cycling chaos similar to that in Figure 2 can be found for the phase-resetting model and the resonance occurs at the same value of γ_c given by (3) and shown in Figure 3. The only difference from the free-running version is that each portions of chaotic trajectory in the active phases now begin in the same way. The main difference between the two models comes in the behaviour as the cycling loses stability at resonance. In the phase-resetting case, the attracting cycle loses stability not to stuck-on chaos but to many co-existing periodic orbits. One such periodic orbit is shown in Figure 6.

3.4. APPROXIMATION OF THE PERIODIC ORBITS NEAR RESONANCE

The nature of the resetting allows us to predict where periodic orbits are likely to occur without having to compute them using the full three-dimensional map. We do this by considering the evolution of the variables over one third of a periodic orbit of period $3N$ as shown in Figure 7, following the method outlined in (Ashwin et al., 2002). We assume that x has just reset to $x_n = \eta$ at $n = 0$, so that y is in the active phase and

z is decaying. For a periodic orbit of period $3N$, we require that $z_N = \eta$ – this will occur when the previous iterate, $z_{N-1} \in [\epsilon, f(\epsilon)]$. We take $y_k = \alpha$, where α is either some $O(1)$ number $\bar{A}$ (for a rough estimate), or more precisely takes the value $f^{N+k}(\eta)$ (since $y_0 = x_N \approx f^N(\eta)$). There follows N iterates of forced decay. We approximate this by $y_{N+k} = r^N y_k e^{-\gamma N\beta}$, where β approximates the suppressing effect of the forcing. Again, for a rough estimate, we take β to be the long-term average A_∞, but for a more accurate estimate we take β to be the N-average $A_N = \frac{1}{N}\sum_{i=0}^{N-1} f^i(f^k(\eta))$. Since this is a periodic orbit, $y_{N+k} = z_k = r^N \alpha e^{-\gamma N\beta}$. Finally we have $(N-k-1)$ iterates of growth, approximated by $z \to rz$. This gives $z_{N-1} = r^{2N-k-1}\alpha e^{-\gamma N\beta}$. Taking logarithms, this estimate predicts that a periodic orbit can exist when

$$\ln\epsilon < (2N-k-1)\ln r + \ln\alpha - \gamma N\beta < \ln\epsilon + \ln r.$$

Taking the rough estimates $\alpha = \bar{A}$, $\beta = A_\infty$ gives a pair of hyperbolae (as discussed in (Ashwin et al., 2002)), given by

$$N \in [N_1, N_2] = \left[\frac{a}{2\ln r - \gamma A_\infty}, \frac{a+\ln r}{2\ln r - \gamma a_\infty}\right] \tag{5}$$

where $a = \ln\epsilon - \ln\bar{A} + (k+1)\ln r$. We expect periodic orbits to exist for values of N lying between these two hyperbolae. The results in (Ashwin et al., 2002) illustrate that this is indeed the case for values of r giving fixed points and periodic solutions within the active invariant subspace, for a suitable choice of fitting parameter $\bar{A}$. Moreover, since the denominators in these expressions equals zero when $\gamma = 2\ln r/A_\infty = \gamma_c$, we can see that the period of the periodic orbits approaches infinity as the coupling parameter approaches the critical value γ_c.

For values of r giving chaotic dynamics within subspaces, the bifurcation diagram of periodic orbits approaching resonance gets more complicated, and the estimate (5) has larger error. We turn to the more sophisticated estimate given by $\alpha = f^{N+k}(\eta)$, $\beta = A_N$ and get

$$z_{N-1} = r^{2N-k-1} f^{N+k}(\eta) e^{-\gamma N A_N}.$$

This is a function only of N (for fixed parameters) and so a curve of z_{N-1} can be easily computed and plotted. Now the method predicts that a periodic orbit can exist for each N for which the curve of z_{N-1} falls within the band given by $[\epsilon, f(\epsilon)]$. The success of this approximation is again illustrated in (Ashwin et al., 2002). Using this method also demonstrates that we expect to find periodic orbits of increasing period as we approach γ_c, and moreover, for the chaotic case, that we may expect periodic orbits to persist even beyond resonance.

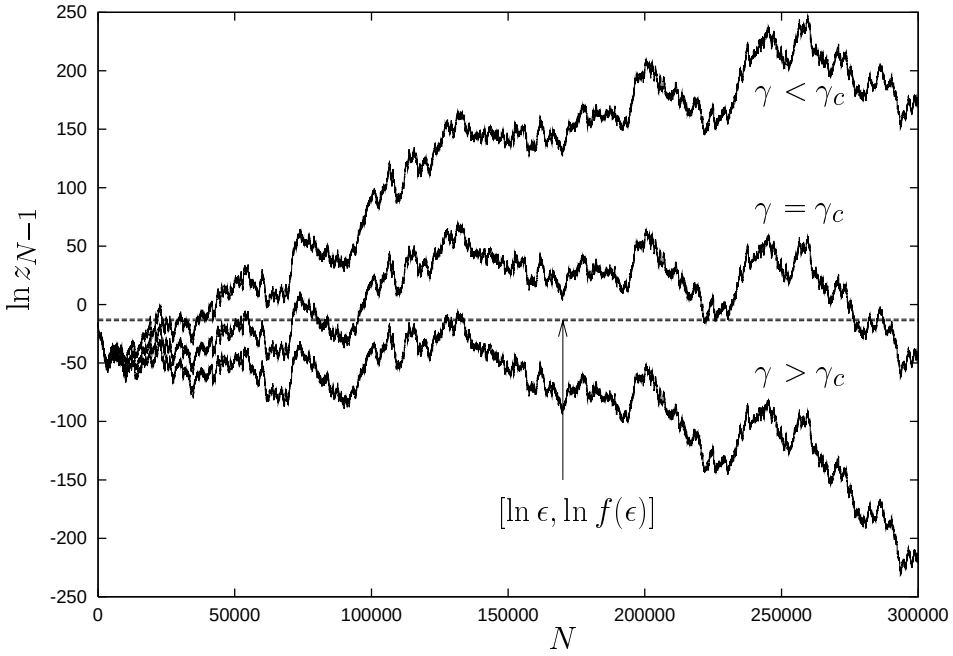

Figure 8. Curves of $\ln z_{N-1}$ given for three different values of γ: a) $\gamma = 4.060 < \gamma_c$, b) $\gamma = 4.061167 = \gamma_c$, c) $\gamma = 4.062 > \gamma_c$.

Consider the curve of $\ln z_{N-1}$ against N, as illustrated in Figure 8 for values of γ below, equal to, and above γ_c. For $\gamma < \gamma_c$ the fluctuations driven by the NA_N term results in many crossings of the band, but eventually the positive linear average behaviour leads the curve away from the band and the fluctuations are no longer large enough to create more crossings. For $\gamma = \gamma_c$ there is no average increase or decrease, but the mean square fluctuations increase linearly with time in a manner familiar from the central limit theorem. This is to be expected for typical chaotic attractors (Baladi, 2001) and means that the curve repeatedly crosses the band, resulting in stable periodic orbits of arbitrarily high period. For $\gamma > \gamma_c$ the negative linear average again leads the curve away from the band, but for values of γ very close to γ_c the possibility of a crossing before the curve is forced too far away remains, and with it the chance of finding periodic orbits persisting beyond resonance.

Figure 9 shows a bifurcation diagram of stable periodic orbits approaching resonance. The lines give the envelope of predicted periodic orbits – the initial and final times the approximation z_{N-1} falls into the band. In between, the dots representing numerically located periodic orbits lie in a complicated structure, but still the approximation works well. In particular

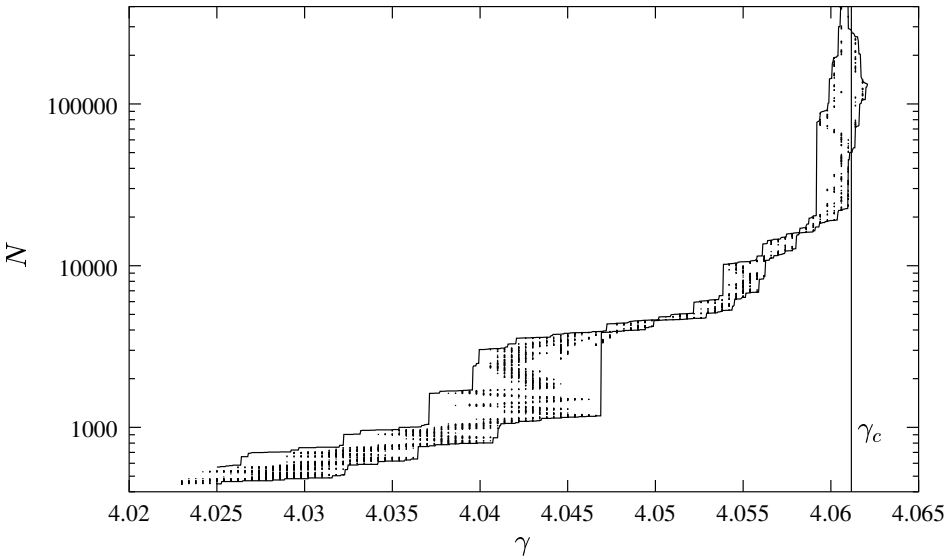

Figure 9. Bifurcation diagram of period $3N$ stable periodic orbits (marked with dots) for $r = 3.75$. The lines show the predicted envelope on varying the parameter γ for the periods computed. The period of the periodic orbits approaches infinity as γ approaches $\gamma_c \approx 4.061165$. Stable periodic orbits can be seen to persist beyond the resonance point.

just beyond γ_c we see the predicted envelope protrudes past the resonance, and indeed one can locate stable periodic orbits for these parameter values, although most initial conditions appear to lead to cycling chaos instead. This is reminiscent of the phenomenon in Shilnikov-type chaos (for example, see (Guckenheimer and Holmes, 1983)) in which stable horseshoes are observed to exist for parameters on both sides of a homoclinic orbit to a spiral saddle, and also to the similar phenomena observed near cycles to heteroclinic cycles (Chawanya, 1999).

If we examine the geometrical rate R of increase (4) of switching time as approximated by $R_n = T_{n+1}/T_n$, we observe a difference in behaviour between the free-running and phase-resetting versions of the system. This is illustrated in Figure 10 where we record the ratio of the number of iterations between successive switches. Before resonance, the phase-resetting model exhibits periodic orbits and so as expected (after transients have died down) this ratio tends to unity as the number of iterations between switches becomes constant. (There are also cases where this can tend to a periodically varying function with unit mean in case the periodic orbit modulo the symmetry does not repeat after N iterates but rather after a multiple of N iterates.) The oscillations in the ratio as the periodic orbit is approached were also seen in the flow example of (Ashwin and Rucklidge, 1998). Conversely, for the free-running case we see the ratio fluctuates as a

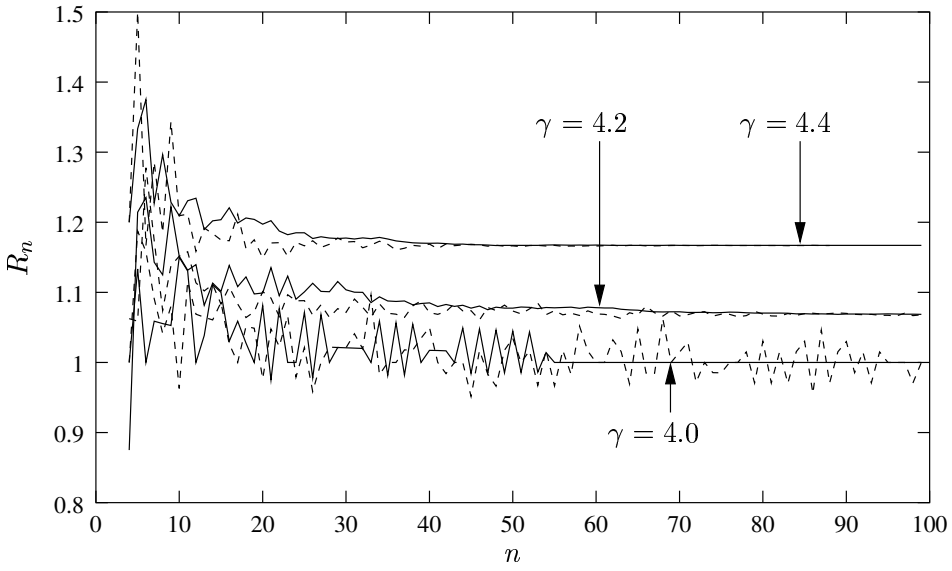

Figure 10. The ratio $R_n = T_{n+1}/T_n$ of number of iterations T_n between switches, n, for the phase-resetting model (solid lines), and the free-running model (dashed lines). The lower pair show a parameter before resonance ($\gamma = 4.0$), giving unity for the periodic orbits in the phase-resetting case, and irregularity for the stuck-on chaos in the free-running model. The other pairs show the free-running model converging more slowly than the phase-resetting model to a geometric increase ($\gamma = 4.2$ and 4.4). The parameter $r = 3.75$ for all pairs.

trajectory follows the irregular cycling of stuck-on chaos.

Beyond resonance, the ratios for both models tend to the same limit R as expected; the convergence appears to be less uniform for the free-running model because of different approaches to the invariant subspaces after each switch; however this is misleading as for example if we choose a value of η for the phase-resetting shelf that has a non-generic orbit this could lead to atypical behaviour for arbitrarily long periods on the cycle.

3.5. SMOOTH MAP WITH PHASE-RESETTING

The map introduced in (Ashwin et al., 2002) and discussed in the previous section could be criticized as being degenerate in the phase-resetting case; it has a flat discontinuous 'shelf' introduced to force the growing phase onto a specific trajectory. We show here that it is a straightforward matter to create a similar map that is arbitrarily smooth. For the growing phase we replace the logistic function $f(x)$ within the interval $[\epsilon, f(\epsilon)]$ by a function which joins on as smoothly as possible at both $x = \epsilon$ and $x = f(\epsilon)$, but which has as small a derivative as possible for as much as possible of the

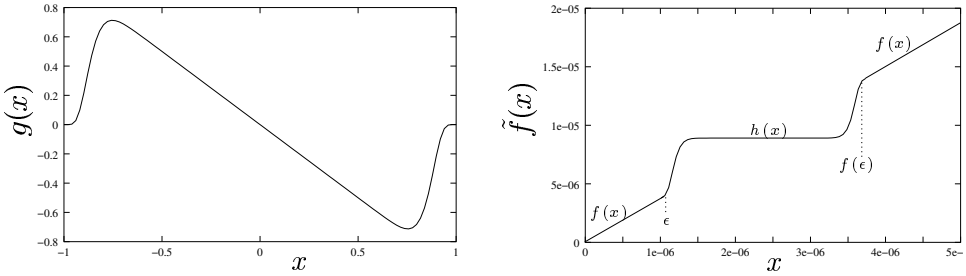

Figure 11. The functions $g(x)$ and $\tilde{f}(x)$ for $p = 9$. This is a smoothed version of the 'shelf' resetting in Figure 5.

interval. To create such a function consider the polynomial

$$g(x) = -x(1 + x^p)^p(1 - x^p)^p$$

for integer values of p. This has zero derivative at $x = \pm 1$, and derivative -1 at $x = 0$. Next we combine $g(x)$ with the logistic map to form a function $h(x)$, valid in the interval $[\epsilon, f(\epsilon)]$, such that $h(\epsilon) = f(\epsilon)$, $h(f(\epsilon)) = f(f(\epsilon))$, and also all the first p derivatives of h and f match up at ϵ and $f(\epsilon)$:

$$h(x) = f(x) + Bg(\phi(x)).$$

The function $\phi(x)$ is chosen to rescale ϵ and $f(\epsilon)$ to -1 and $+1$ respectively (that is, $\phi(x) = mx + c$, where $m = 2/(f(\epsilon) - \epsilon)$, and $c = -1 - m\epsilon$), and B is chosen to ensure $h'((\epsilon + f(\epsilon))/2) = 0$, to give a flat shelf. The higher the value of p chosen, the longer and flatter the shelf. Finally, the phase-resetting function $\tilde{f}(x)$ is created by combining $f(x)$ and $h(x)$ according to

$$\tilde{f}(x_n) = \begin{cases} f(x_n) & x_n < \epsilon \text{ or } x_n > f(\epsilon) \\ h(x) & x_n \in [\epsilon, f(\epsilon)]. \end{cases}$$

The behaviour in this continuous version of the phase-resetting model combines properties from both the free-running and the original phase-resetting maps. Again the critical value of γ marking the onset of stability of cycling chaos can be found as before. Decreasing γ through γ_c we find that cycling chaos gives way to stuck-on chaos, just as in the free-running example above. However, decreasing γ results in the stuck-on chaos being replaced by stable periodic orbits, as found in the phase-resetting example. Figure 12 illustrates these transitions by showing (as in figure 10) the rate of increase of switching times $R_n = T_{n+1}/T_n$. First in graph (a) for $\gamma = 3.87$ (far from $\gamma_c \approx 4.0116$), R_n tends to unity after quite a long transient. This indicates presence of a periodic orbit that closes after a single circuit of the cycle (in this case the period is $N = 35$). Increasing to $\gamma = 4.0$ leaves

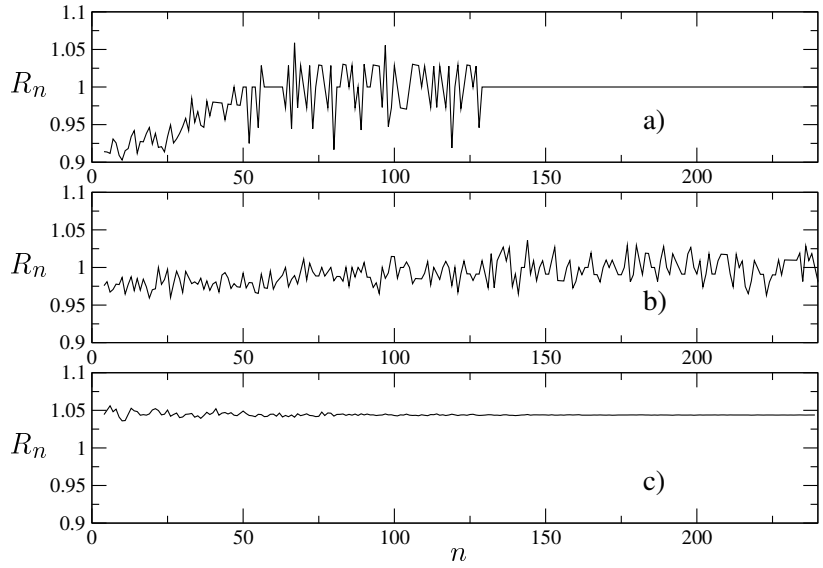

Figure 12. The ratio $R_n = T_{n+1}/T_n$ of number of iterations T_n between switches n for the smooth phase-resetting model. All graphs have $p = 79$ and $r = 3.75$. The top graph a) shows the ratio converging to unity, as a periodic orbit is reached for $\gamma = 3.87$. The middle graph b) shows the irregularity of stuck-on chaos obtained from $\gamma = 4.0$. Finally the bottom graph c) shows the geometric increase of cycling chaos beyond the resonance for $\gamma = 4.15$.

the system in a state of stuck-on chaos, shown in graph (b) by the ratio fluctuating about an average of unity. Finally in graph (c) the ratio tends to 1.0437 giving, for the post-resonance case $\gamma = 4.2$, the exponent of the geometric increase of switching times associated with cycling chaos.

4. Conclusions

In this work we have briefly reviewed some effects of symmetries on dynamics of coupled cell networks and synchronization. We have also extended (Ashwin et al., 2002) in a number of ways: firstly by considering the ratio of geometric slowing-down for the phase-resetting and free-running cases; and secondly by adapting the phase-resetting case to show that the discontinuity is not essential to give phase-resetting effects.

The model in itself can be interpreted as a ring of mutually-inhibiting cells, and exhibits non-ergodic and intermittent attracting behaviour familiar for robust cycles (Krupa, 1997) and 'cycling chaos' (Dellnitz et al., 1995).

The scenario for loss of stability of a cycle in a flow as investigated in (Ashwin and Rucklidge, 1998) has addition problems in that there is no global section to the attractor and the equilibria are contained within the subspaces that contain the chaotic attractors but nonetheless the maps with singularities appear not to be a bad approximation. In the former model the cycle is formed between alternating saddle equilibria and chaotic saddles, and the phase resetting is caused by the fact that the connection from equilibrium to chaos was along a one-dimensional unstable manifold. This can clearly be robust within an invariant subspace. If we try to make a global section to the flow, near the cycling chaos this will give rise to, at best, a return map that has infinite time of return near the cycle itself and a singularity in the map near the stable manifold of the equilibrium.

In conclusion, there seems to be a lot of promise to understand a wide variety of very complicated but robust intermittent dynamical states in networks of coupled cells by exploiting and adapting tools from dynamical systems with symmetries.

Acknowledgments

The research of PA, AR and RS was supported by EPSRC grant number GR/N14408. We thank Arkady Pikovsky for some pertinent questions relating to cycling chaos.

References

P. Ashwin, Cycles homoclinic to chaotic sets; robustness and resonance. *Chaos* **7** 207–220 (1997)

P. Ashwin, Chaotic intermittency of patterns in symmetric systems. *Proceedings of IMA workshop on pattern formation in coupled and continuous systems.* Editors: M Golubitsky, D Luss and S H Strogatz, IMA volumes in Mathematics and its applications 115, Springer (1999)

P. Ashwin, J. Buescu and I.N. Stewart, Bubbling of attractors and synchronisation of chaotic oscillators, *Physics Letters A* **193** 126-139 (1994)

P. Ashwin and M. Field. Heteroclinic networks in coupled cell systems. *Arch. Rational Mech. Anal.* **148** 107–143 (1999)

P. Ashwin, A. M. Rucklidge and R. Sturman, Infinities of periodic orbits near robust cycling. In press, *Phys. Rev. E* (2002)

P. Ashwin and A. M. Rucklidge, Cycling chaos; its creation, persistence and loss of stability in a model of nonlinear magnetoconvection. Physica D **122** 134–154 (1998)

V. Baladi, Decay of correlations, In *Smooth ergodic theory and its applications (Seattle, WA, 1999)* pp 297–325, Amer. Math. Soc., Providence (2001)

T. Chawanya, Coexistence of infinitely many attractors in a simple flow. *Physica D* **109** 201–241 (1997)

P Chossat, M Krupa, I Melbourne and A Scheel, Transverse bifurcations of homoclinic cycles. Physica D **100** 85–100 (1997)

P Chossat, M Krupa, I Melbourne and A Scheel, Magnetic dynamos in rotating convection - A dynamical systems approach. Dynamics of Continuous, Discrete and Impulsive Systems **5** 327–340 (1999)

S-N Chow, B Deng and B Fiedler, Homoclinic bifurcation at resonant eigenvalues. *J. Dyn. Diff. Eqns.* **2** 177–244 (1990)

M. Dellnitz, M. Field, M. Golubitsky, A. Hohmann and J. Ma, Cycling Chaos. *I.E.E.E. Transactions on Circuits and Systems: I. Fundamental Theory and Applications*, **42** 821–823 (1995)

A. Gaunersdorfer, Time averages for heteroclinic attractors, *SIAM J. Appl. Math.* **52** 1476–1489 (1992).

M. Golubitsky and D. Schaeffer, *Singularities and Groups in Bifurcation Theory, Vol 1.* Springer Applied Math. Sci. vol 51 (1985).

M. Golubitsky, I. Stewart and D.G. Schaeffer, *Singularities and Groups in Bifurcation Theory, Vol 2* . Springer Applied Math. Sci. vol 69 (1988).

M. Golubitsky and I. Stewart, *From Equilibrium to Chaos in Phase Space and Physical Space* Birkhauser, Basel, (2002).

J. Guckenheimer and P. Holmes, *Nonlinear oscillations, dynamical systems and bifurcations of vector fields,* Applied Mathematical Sciences **42**, Springer Verlag, (1983)

J. Guckenheimer and P. Holmes, Structurally stable heteroclinic cycles, *Math. Proc. Camb. Phil. Soc.* **103** 189–192, (1988)

J. Hofbauer and K. Sigmund, *The Theory of Evolution and Dynamical Systems*, Cambridge University Press, Cambridge, (1988)

K. Kaneko, On the strength of attractors in a high-dimensional system: Milnor attractor network, robust global attraction, and noise-induced selection. *Physica D* **124**, 308-330 (1998)

M. Krupa, Robust heteroclinic cycles, *Journal of Nonlinear Science* **7** 129–176 (1997)

J. Kurths and S.A. Kuznetsov, *preprint* (2001)

E. Ott and J. C. Sommerer, Blowout bifurcations: the occurrence of riddled basins and on-off intermittency. *Phys. Lett. A* **188** 39–47 (1994)

A. Pikovsky, O. Popovych and Yu. Maistrenko, Resolving clusters in chaotic ensembles. *Phys. Rev. Lett.*, **87** 044102 (2001)

K. Sigmund, Time averages for unpredictable orbits of deterministic systems, *Annals of Operations Research* **37** 217–228 (1992)